RESEARCH ARTICLE

Toxicity Evaluation of Silver Nanoparticle in the Kidneys of Wistar Rats

Anita K Patllola[1,2*], S Anitha Kumari[3], Zada Lusk[2,4]

Abstract

This study aimed to evaluate the nephrotoxic effects of silver nanoparticles (AgNPs) in Wistar rats using biochemical, oxidative stress and histopathological changes. Three groups of six rats were orally administered AgNPs once a day for 28 days with doses of 100, 500, 1000 mg/kg bodyweight. A control group was administered with deionized water. Blood and kidneys were collected 24 hours after the last treatment following standard protocols. The activities of creatinine and blood urea nitrogen against AgNP-induced toxicity was determined in the serum by colorimetric microplate assay. Various activity levels of oxidative stress including, Catalase (CAT), Superoxide dismutase (SOD), Glutathione peroxidase (GPx) and Lipid hydroperoxides (LPO) were evaluated in the kidney tissue. Scanning (SEM) and transmission electron microscopy (TEM) was used to determine the histopathological evaluation of the kidneys. A significant increase in the levels of serum creatinine, blood urea nitrogen, CAT and LPO, were noted in AgNPs exposed rats compared to that in control rats. In contrast, decreased activities of SOD and GPx in a dose-dependent manner was observed in AgNPs exposed rats relative to control rats. SEM and TEM study showed significant morphological alterations in kidneys of AgNPs exposed rats in accordance with the biochemical markers. The results of the study demonstrate that AgNPs might be nephrotoxic, and its toxicity is mediated through oxidative stress mechanism.

Key Words: *Silver nanoparticles; Serum creatinine; Blood urea nitrogen; Oxidative stress; Wistar rats*

[1]*NIH-Center for Environmental Health, College of Science, Engineering and Technology, Jackson State University, Jackson, MS, USA*

[2]*Department of Biology, Jackson State University, Jackson, MS, USA*

[3]*Department of Zoology, Nizam College, Basheer Bagh, Hyderabad, India*

[4]*Thee Aristocrats STEM & health Science Program, Jackson State University, Jackson, USA*

[*]Corresponding author: Anita K Patlolla, Assistant Professor, CSET, 1400 Lynch Street, PO. Box 18540, Jackson State University, Jackson, MS 39217, USA, Tel: +601 979 0210; Email: anita.k.patlolla@jsums.edu

Introduction

Nanotoxicology is the study of how living organisms, and the environment are affected by manufactured nanomaterials. In various fields, such as industrial applications, biological and biomedical science [1], healthcare technology, and household appliances, there is an increasing demand for nanoparticles [2-5]. With the increasing presence of AgNPs in commercial products, there is growing concern about potential poisoning, but toxic evidence on AgNPs is still not available. Analyzing the biochemical parameters can help identify the target organs for toxicity, reveal the general health status of animals and contribute to an advance information of stress in organisms.

Silver nanoparticles (Ag-NPs) also known as nano-silver possess unique physico-chemical properties [6], regarded as the best known nanoproducts [7] and have been used in several applications [8]. With the increasing use of Ag-NPs, the public has a higher risk of exposure in daily life, through occupational environments and consumer products. Additionally, the adverse effects of Ag-NPs on human health and the environment are of increasing concern [9]. AgNPs can easily enter the human body due to their size via ingestion [10], inhalation [11] as well as skin contact [12]. The various organs such as kidneys, lungs, nervous system, and liver are more prone to the accumulation of AgNPs [13,14]. Besides the directly exposed tissues, AgNPs can also be transported via blood circulation to different organs [14]. Further, several investigations have demonstrated that the silver ions released from the ingested products into the blood accumulate in the body organs causing toxic effects in the organs particularly in the liver and kidney [15]. AgNPs are reported to be more toxic than the other nanoparticles including aluminium, nickel, iron, and manganese [16]. However, the mechanism of their toxicity is not clearly known.

The kidneys obtain just about 20% of the whole cardiac output despite their small size making the organ highly exposed to xenobiotics such as NPs [17]. Since the key important function of the kidneys is to eliminate the metabolic waste and a variety of potentially harmful substances including the excretion of NPs these organs are the important targets for investigation about nanoparticle exposure and hazard [18]. Kidneys possess active oxidative metabolism that results in ROS generation which can damage the major cellular components. The free radicals that are produced affect the cell integrity producing the peroxidation of lipids in the intracellular membranes and cross linking with the macromolecules in the membranes. Furthermore, creatinine and urea are significant indicators of renal function [19,20]. Owing to the increasing rate of applications in medicine and the widespread availability of AgNPs in the environment, its safety on the mammalian renal system should not be assumed [21,22].

This study provides a comprehensive overview of the toxicity evaluation of silver nanoparticles on Wistar rats, including the lipid hydroperoxide assay, and the histopathological evaluation. Hence the assessment of the harmful effects of AgNPs is conducted by measuring the creatinine and urea levels in the serum sample. The induction of oxidative stress was determined by measuring the activities of catalase, superoxide dismutase, glutathione peroxidase and lipid hydroperoxides. Furthermore, to get insight of the morphological alterations, both scanning and transmission electron microscopical examination of the kidney tissue was carried out in both exposed and control rats.

Material and Methods

Chemicals

Silver nanoparticles with a particle size of less than 100 nm were purchased from Sigma-Aldrich (ST. Louis, MO, USA. All the other chemicals used in the present study were of Analytical grade and purchased from Sigma-Aldrich, (St. Louis, MO, USA). CAT, SOD and LPO kits were obtained from Calbiochem (CA).

TEM analysis

Transmission electron microscope (TEM) was used to determine the size, shape, and morphology of the silver nanoparticles. The samples of sonicated pellet of centrifuged AgNPs in deionized water were used for TEM analysis. On a carbon-coated copper grid, a drop of the homogenous suspension was placed with a lacey carbon film and allowed to dry at room temperature. The images were collected using a field emission JOEL-JEM-2100F TEM operating at 200 kv (JOEL-Tokyo, Japan).

Dynamic Light Sacttering (DLS)

The nanostructure, size and zeta potential were measured in deionized water (DI) following manufacturer's protocol using a Zetasizer (Malvern, Worcestershire, UK).

Treatment of animals

Six to eight weeks old male Wistar (Albino) rats weighing between 100-150 grams were purchased from National Institute of Nutrition (Hyderabad, India). The rats were fed on commercial pellet diet and water-ad-libitum and were allowed to acclimate to the laboratory conditions for 1 week prior to the experimentation. The rats were divided into 4 groups of 6 animals each (3 experimental and one control group). Three different concentrations of AgNPs (100,500 and 1000 mg/Kg) were made and administered to the rats orally by gastric intubation. The groups (1 to 3) considered as treated groups were given 100, 500 and 1000 mg/Kg. body weight of AgNPs suspension orally for a period of 28 days following organization for economic-cooperation and development [21], while group 4 considered as control was given deionized water. This study followed the guidelines of IAEC (Institutional Animal Ethics Committee) and the protocol was approved by the local Ethics committee for animal experiments at Nizam College, Hyderabad, India. The doses were selected based on the preliminary acute oral toxicity of AgNPs [23]. Both the control and the treated animals were maintained at a temperature of 22-25^{0}C with relative humidity of 30-70% and 12 hours light and 12 hours darkness respectively. The treated animals were monitored daily for any behavioral changes, food consumption and body weight. After 24 hours of last administration of the dose, all the treated animals along with the control were sacrificed by cervical dislocation and the blood samples were collected immediately from the ventricle through cardiac puncture by disposable syringe. The blood was allowed to clot at room temperature and the serum was separated by centrifugation at 1500 g for 10 minutes and used for the estimation of creatinine and blood urea. Simultaneously the kidney tissue was removed and rinsed with the saline solution (0.9% NaCl) for the evaluation of oxidative stress. The kidney tissue was removed, weighed, and homogenized. About 10% of the tissue homogenate was prepared separately in 0.05 M phosphate buffer (P^H 7.4) containing 0.1 mM EDTA using a homogenizer followed by sonication and centrifugation at 500× g for 10 minutes at 4^{0}C. Further, the supernatant was decanted and centrifuged at

2000× g for 60 minutes at 4⁰C. The cellular fraction thus obtained is used for the assay of Catalase (CAT), Superoxide dismutase (SOD), Glutathione Peroxidase (GPx) and Lipid hydroperoxides (LPO).

Serum creatinine assay

Serum creatinine was determined following the procedure adopted from the method of Folin and Wu, described in Hawk, by Oser and Summerson. The method is based on Jaffe reaction where creatinine reacts with the picrate ion formed in an alkaline medium to develop a red-orange color. The color produced from the sample is compared with that produced by a known amount of creatinine under the same condition in a colorimeter at a wavelength of 505nm. To prepare 1 mM (1n mole/mL) standard solution, about ten milliliters of 100 mM (100 nmole/mL) of creatinine standard solution was added to 990 mL of creatinine assay buffer.

Then 0,2,4,6,8 and 10 mL of 1 mM creatinine standard solution was added into a 96 well plate generating O (blank), 2,4,6,8 and 10n mole/well standards. The creatinine assay buffer was added to each well to make the volume 50 mL. Fifty milliliters of the reaction mixture were added to each of the wells and mixed using a horizontal shaker or by pipetting followed by incubation at 37⁰C for 60 minutes. The absorbance was measured at 570 nm (A570). The concentration of creatinine was calculated using the formula.

$C = Sa/Sv$

Sa = Amount of creatinine in unknown sample (n mole) from standard curve.

Sv = Sample volume (mL) added into the wells.

C = Concentration of creatinine in sample.

Blood urea nitrogen assay

The blood urea nitrogen was determined using the Max Discovery blood urea nitrogen enzymatic kit (BIOO Scientific, Austin, Texas, USA) which measures the concentration of urea using the urease enzyme that converts urea to ammonia.

$$CO(NH_2) + H_2O \xrightarrow{urease} CO_2 + 2NH_3$$
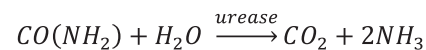
It is a microplate-based colorimetric assay used for the determination of urea in the serum sample. About 0.2-1 ml of blood sample were allowed to coagulate in a micro-centrifuge tube at 37⁰C for 20 minutes and then centrifuged at 9000 rpm for 5 minutes. The supernatant (serum) thus obtained was transferred to a clean tube. Then the serum sample was diluted to 1:4 ratio in either normal saline or phosphate buffer saline (PBS) (dilution factor=5). About 5 µL of the diluted serum was added to the microplate wells in duplicate followed by the addition of 150 µL of the urease mix solution. The plate was then gently tapped 3-4 times for proper mixing of the sample and the enzyme and was incubated at room temperature for 15 minutes. Then about 150 µL of alkaline hypo chlorite solution was added to each well and incubated at room temperature for 10 minutes. The absorbance of each sample was measured in duplicate at 620 nm. A calibration curve of urea standards was then used to determine the concentration of urea in the samples. The blood urea concentration (dilution factor) in the well can be determined using the equation.

Blood urea concentration = dilution factor × (Average absorbance-Y intercept) slope

Catalase (CAT) assay

The catalase activity in the kidneys was determined following the method of [24]. In brief, the kidney tissues were rinsed with phosphate buffer, P^H (7.4) to remove the excess

amount of blood and were homogenized (1:8 w/v) in cold buffer containing 50 mM potassium phosphate, P^H 7.0 and 1mM ethylene diamine tetra acetic acid (EDTA) per gram tissue. Then the supernatant was used as the enzyme source and analyzed with 96 well plates using the commercial catalase assay kit. The method is based on the reaction of catalase with methanol in the presence of an optimal concentration of H_2O_2 and the formaldehyde produced was measured. Three replicates of 20 µL sample were taken and mixed with 100 µL of 100 mM potassium phosphate (P^H 7.0) and 30 µL of methanol. The reaction was initiated by adding 20 µL of 35 mM hydrogen peroxide followed by incubation of the mixture on shaker for 20 minutes at room temperature. The reaction was then terminated by adding 30 µL of 10 M potassium hydroxide. About 30 µl of 4-amino-3-hydrazino-5-mercapto-1,2,4-triazole was added to the three replicates of each sample and then incubated on a shaker at room temperature for 10 minutes. After incubation, about 10 µl of Calbiochem supplied potassium periodate was added to the mixture and again incubated at room temperature for 5 minutes. Finally, the absorbance of the reaction mixture was recorded at 540 nm using 96 well plate reader. A reference standard was prepared using formaldehyde solution.

Superoxide Dismutase (SOD) assay

The SOD activity in the kidneys was analyzed following the method of [25]. The method is based on the utilization of a tetrazolium salt for detection of superoxide radicals generated by xanthine oxidase and hypoxanthine. In brief, the tissues were rinsed with phosphate buffer (P^H 7.4) containing 0.16 mg/ml heparin to remove the excess amount of blood. The tissues were then homogenized (1:8 w/v) in cold 20 mM HEPES buffer (P^H 7.2) containing 1 mM EGTA, 210 mM mannitol and 70 mM sucrose per gram tissue. The tissue homogenate was centrifuged at $1500\times$ g at 4^0C for 5 minutes and the supernatants were analyzed with 96 well plate using the commercial SOD assay kit. Three replicates of 10 µL of each sample were taken and mixed with 200 µL of radical detector. The radical detector was prepared using 50 µL of Calbiochem supplied tetrazolium salt solution and 19.95 mL of 50 mM Tris-Hcl (P^H 8.0) containing 0.1 mM diethylenetriamine penta acetic acid (DTPA) and 0.1mM hypoxanthine. The reaction was then initiated by adding 20 mL of xanthine oxidase followed by incubation of the reaction mixture on a shaker at room temperature for 20 minutes. The xanthine oxidase was prepared using 50 µL of Calbiochem suppled xanthine oxidase solution and 1.95 mL of 50 mM Tris-HCl (P^H 8.0). After incubation, the absorbance of the reaction mixture was measured at 450 nm using 96 well plate reader. The standard reference curve was prepared using the solution of bovine erythrocyte SOD.

Glutathione Peroxide (GPx) assay

The GPx activity in the kidney tissue was determined following the method of [26]. The method indirectly measures the GPx activity by a coupled reaction with glutathione reductase. In brief, the kidney tissues were perfused with phosphate buffer saline (PBS), (P^H 7.4) containing 0.16 mg/mL heparin to remove the excess blood. The tissues were then homogenized (1:8 w/v) in cold homogenizing buffer containing 50 mM Tris-Hcl (P^H 7.5), 5mM EDTA and 1mM DTT per gram tissue. The homogenates were centrifuged at 10,000$\times$ g at 4^0C for 15 minutes and the supernatants were separated. Three replicates of 20 µL of each sample was then mixed with 100 µL of 50 mM Tris-HCl (p^H 7.6) containing 5mM EDTA and 50 µL of co-substrate mixture (Calbiochem supplied NADPH, glutathione, and glutathione reductase). Further, the reaction was initiated

by adding 20 µL of cumene hydroperoxide solution. The reaction mixture was mixed well, and the absorbance was recorded at 340 nm.

Lipid Hydroperoxide (LPO) assay

The LPO activity in the kidney tissue was analyzed using the commercial LPO assay kit. The method directly measures the lipid hydroperoxides utilizing redox reactions with ferrous ions. The produced hydroperoxides are highly unstable and thus react readily with the ferrous ions to form ferric ions, which are detected using thiocyanate ion as chromogen. The Calbiochem supplied lipid hydroperoxides solution was used as a reference standard. Briefly, the kidney tissues were homogenized (1:8 w/v) in cold HPLC grade water. Then about 500 µL of each tissue homogenate was taken in a test tube and equal volume of Calbiochem supplied Extract R saturated methanol was added to it. The mixture was then vortexed for a few minutes and 1mL of cold deoxygenated chloroform was added to it and again vortexed thoroughly. The mixture was centrifuged at $1500 \times$ g at 0^0C for 5 minutes and the bottom chloroform layer was collected. About 500 µL of the bottom chloroform was mixed with 450 µL of chloroform: methanol (2:1) mixture and 50 µL of Calbiochem supplied thiocyanate ion (chromogen). The mixture was then incubated for 5 minutes, and the absorbance of each sample was measured at 500 nm wavelength using a spectrophotometer.

Statistical analysis

One-way analysis was used for the comparison of the data through Statistica version 5.0 (Statsoft, India). The results were expressed as Mean ± S.D. The value of $p < 0.05$ was considered statistically significant.

Histopathological Evaluation

Sample preparation for Scanning Electron Microscope (SEM) study

The collected kidney tissue from both control and treated rats were washed in normal saline to remove the excess blood and fixed in cold Karnovsky fixative [27,28].

After one hour, the kidney tissue is cut into small slices of about 10-50 nm size and fixed in fresh cold Karnovsky fixative for overnight at 4^0C. Then the samples were washed 3 times with 0.2 M sodium cacodylate buffer with 30 minutes interval and post fixed with 2% buffered osmium tetroxide for 2 hours at 4^0C, washed again in SCB 3 times with 30 minutes interval and dehydrated by passing through ascending grades of ethanol, from 30% to 100% at 4^0C for one hour. Then 100% ethanol was added again to the tissue samples and kept for another hour at room temperature for complete dehydration. Then the samples were removed from 100% ethanol and air dried under high vacuum (10^{-7} Torr) at room temperature (25^0C) for one day followed by treatment of the tissue sample with HMDS (1.1.1.3.3.3 Hexa Methyl Disilazane) and dried under vacuum for 2 hours to complete drying [29]. The dried tissue samples were mounted on aluminum stub with double sided adhesive tape and coated with ionic gold (300Å) in sputter coating unit E-1010 (Hitachi, Japan) at high vacuum. The processed tissue samples were then scanned under scanning electron microscope (SEM) (S3400N Hitachi, Japan) at 15 kv, and high vacuum (10^{-7} Torr) and scanned pictures were taken in different magnifications.

Sample preparation for Transmission Electron Microscope (TEM) Study

For TEM studies, the collected kidney tissues from both control and treated rats were washed in normal saline to remove excess blood and

fixed in cold karnovsky fixative. After one hour, the kidney tissues were removed and were cut into slices of about 1-10 mm size by using a scalpel blade [30]. The tissue slices were fixed in cold karnovsky fixative for overnight at 4^0C followed by washing 3 times with 0.1 M sodium cacodylate buffer with 30 minutes interval to remove the excess fixative and post fixed with 2% buffered osmium tetroxide for 2 hours at 4^0C. The tissue samples were washed again in SCB 3 times with 30 minutes interval and dehydrated by passing through ascending grades of ethanol from 30% to 90% kept for 30 minutes interval and 100% ethanol for one hour at 4^0C. Then 100% ethanol was added again to the tissue samples and kept for another hour at room temperature for complete dehydration. The dehydrated samples were then cleared in propylene oxide and infiltrated in tandem with propylene oxide and epoxy resin mixture. Then fresh pure resin was added to the samples and kept for 2 hours at room temperature. The samples were further embedded with resin mixtures in plastic beam capsules of 1cm size and polymerized by keeping them in a vacuum oven for 24 hours at 50^0C and for another 24 hours at 60^0C. The prepared blocks were removed from the vials and ultrathin sections of the tissue sample were cut with glass or diamond coated knife using ultramicrotome (Leica Ultracut; UCT-GA, D/E-1600). The cut sections (60-70 nm) were collected and placed on a double coated 200 mesh copper grid and were double stained with uranyl acetate and lead citrate. The sections were analyzed by Hitachi H-7500 Transmission electron microscope (TEM) at 60-80 kv under high vacuum (10^{-7} Torr) and the pictures were taken as per required magnification [31].

Results

Figure 1 represents transmission electron microscope images of the size, shape, and morphology of AgNPs. It showed that silver nanoparticles were well dispersed and predominantly spherical in shape. Figure 2 represents the results from DLS showing the particle size with an average diameter of 39 nm and at least 7 nm diameter respectively.
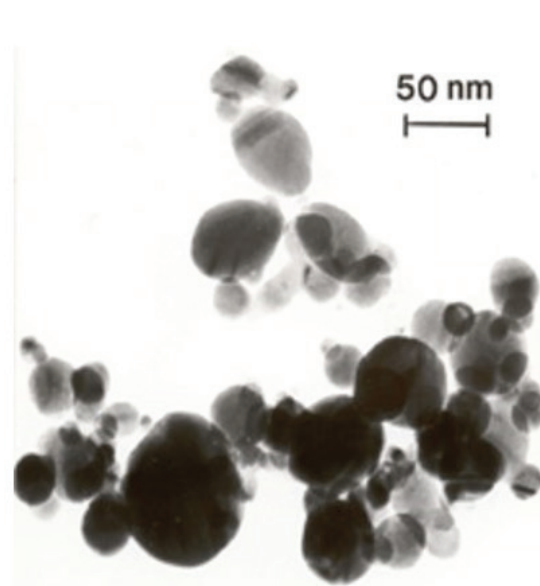
Figure 1) *TEM photo of AgNPs.*

A

B
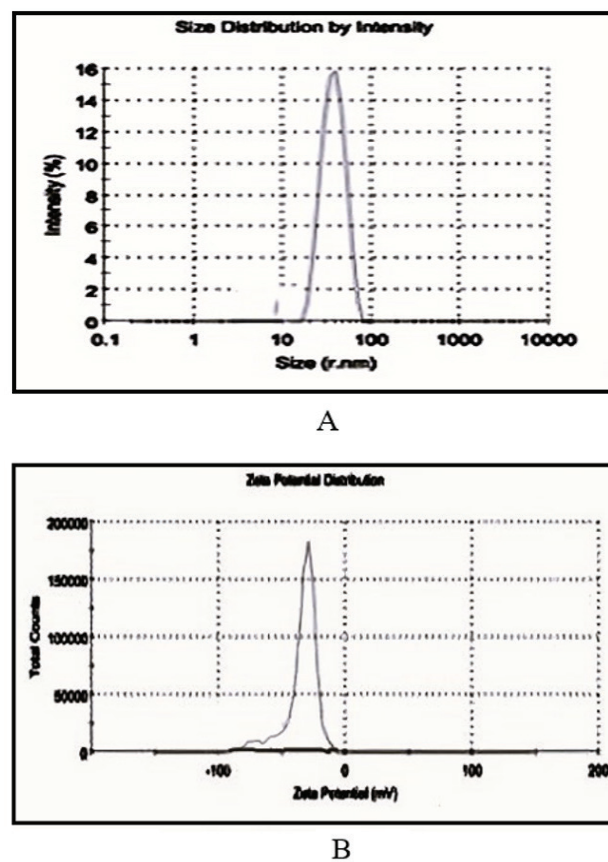
Figure 2) *A) represents the results from DLS showing the particle size with an average diameter of 39 nm and at least 7 nm diameter respectively. B) Zeta potential (33.2).*

Clinical Symptoms, food consumption, body weight, organ weight and general activity

No mortality, gross effects or any significant differences in food consumption or body weight and organ weight were observed in any of the treated rats throughout the experimental period when compared with the control group. However, the treated rats revealed a marked decrease in their activity. The treated rats showed abnormal behavioral patterns such as lethargy and irritation.

Biochemical analysis

Catalase (CAT): The results of the catalase assay are presented in Figure 3. The results showed an increase in the catalase activity in AgNPs treated rats compared to control. The catalase activity was found to be 623.40 ± 6.66 for control and $832.50 \pm 7.20, 1014.90 \pm 8.14$ and 1330.04 ± 10.01 nmole/min/gm/tissue for 100, 500 and 1000mg/kg dose of AgNPs respectively. There was a dose-dependent increase in the catalase activity compared to control. However, statistically significant effect was observed in the highest two doses, 500 and 1000 mg/Kg compared to control.
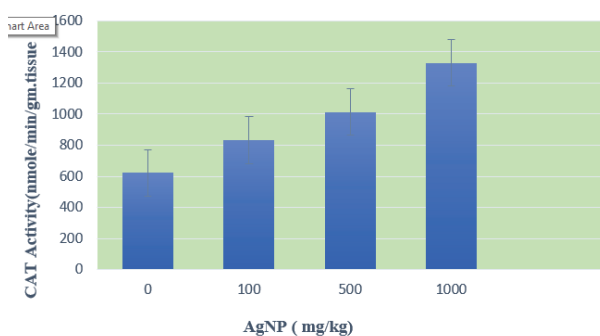
Figure 3) *Effect of silver nanoparticles on the activity of catalase in kidney of Wistar rats. Data represents mean +SD. Statistical significance (p<0.05).*

Superoxide Dismutase (SOD): The results of the SOD activity of control and treated rats of kidney are presented in Figure 4. The SOD activity levels in kidney were 1.64 ± 0.07 for control and 1.02 ± 0.04, 0.69 ± 0.02 and $0.54 \pm$ 0.01 U/gm/tissue for 100, 500 and 1000 mg/kg dose of AgNPs respectively. The SOD activity decreased with the increasing concentration of AgNPs in treated rats compared to control. However, the SOD activity was significantly decreased in the highest two doses, 500 and 1000 mg/Kg treated rats compared to control.
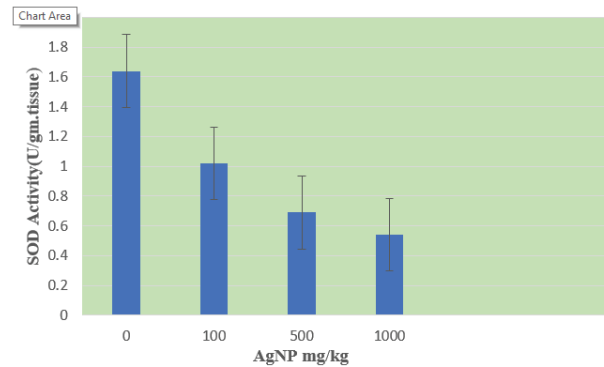
Figure 4) *Effect of silver nanoparticle on the activity of superoxide dismutase in kidney of Wistar rats. Data represents mean +SD. Statistical significance (p<0.05).*

Glutathione Peroxidase (GPx): The results of the glutathione peroxidase activity of control and treated rats are presented in Figure 5. The glutathione peroxidase levels were found to be 38.5 ± 0.38 for control and 30.5 ± 0.25, 25.6 ± 0.17 and 20.10 ± 0.10 nmole/min/gm/tissue respectively for 100, 500 and 1000 mg/Kg dose of AgNPs. The glutathione peroxidase activity in kidneys was found to be decreased in all the treated groups compared to the control group. However, there was a significant decrease in 500 mg/Kg and 100 mg/Kg dose of treated groups compared to the control group.
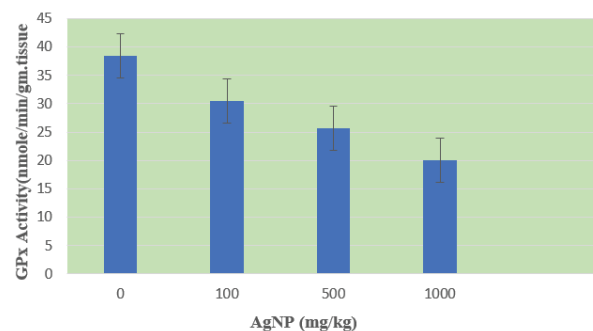
Figure 5) *Effect of silver nanoparticles on the activity of glutathione peroxidase in kidney of Wistar rats. Data represents mean +SD. Statistical significance (p<0.05).*

Lipid Hydroperoxides (LPO): Lipid hydroperoxide assay was performed to determine the hydroperoxide levels in kidney of both treated and control groups. The LPO levels in kidney of treated and control groups are presented in Figure 6 and were found to be 35.70 ± 2.30 for control and 56.18 ± 3.50, 79.10 ± 3.91 and 85.25 ± 4.50 µM/gm/tissue for 100, 500 and 1000 mg/Kg dose of AgNPs respectively. The LPO levels of the kidneys were found to be significantly increased in a dose dependent manner in all the treated groups compared to the control group. However, highly significant increased LPO levels were found in 500 mg/Kg and 1000 mg/Kg dose of treated groups.
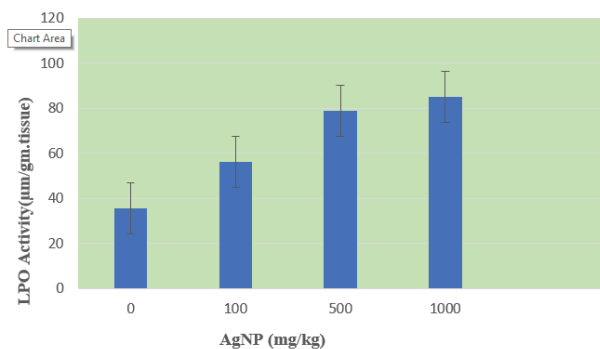
Figure 6) *Effect of silver nanoparticles on the activity of lipid hydroperoxide in kidney of Wistar rats. Data represents mean +SD. Statistical significance (p<0.05).*

Serum Creatinine: The mean values of the serum creatinine are presented in Figure 7. The serum creatinine levels were found to be significantly increased in all the treated groups in a dose- dependent manner when compared to the control group. The results yielded serum creatinine levels of treated rats as 2.35 ± 0.08, 3.64 ± 1.63 and 4.18 ± 1.70 mg/dL for 100, 500 and 100 mg/Kg dose of AgNPs respectively relative to control group (0.70 ± 0.08 mg/dL). as shown in the Figure. There was a significant increase in the serum creatinine levels of treated rats. However, the increase was statistically significant in the highest two doses, 500 and 1000 mg/Kg relative to control.
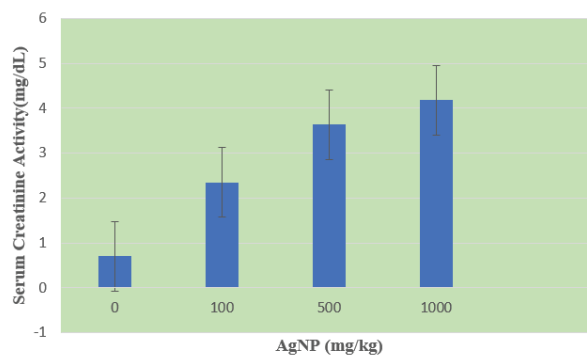
Figure 7) *Effect of silver nanoparticles on the activity of serum creatinine in Wister rats. Data represents mean +SD. Statistical significance (p<0.05).*

Blood urea Nitrogen (BUN): Figure 8 represents the blood urea nitrogen (BUN) in rats exposed to AgNPs. The results of BUN were obtained as 30.17 ± 1.50 for control and 41.0 ± 2.3, 50.0 ± 3.1 and 63.3 ± 4.5 mg/dL for 100, 500 and 100 mg/Kg dose of AgNPs treated rats. Rats exposed to AgNPs elevated the levels of BUN in a dose-dependent manner. However, the increase was statistically significant in the highest two doses, 500 and 1000 mg/Kg dose compared to control.
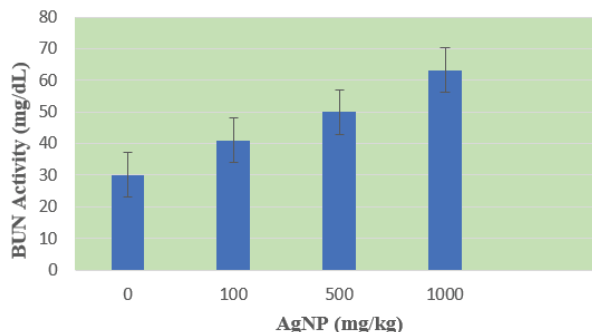
Figure 8) *Effect of silver nanoparticles on the activity of BUN in kidney of Wister rats. Data represents mean +SD. Statistical significance (p<0.05).*

Histopathological evaluation: In the present study, the histopathological evaluation was done using both scanning and electron microscope study. The results of the SEM study are shown in Figure 9 for control and treated rats respectively. The kidney of the control rats showed normal surface architecture when compared with the treated rats. The kidney of the control rats showed normal glomeruli with

blood capillary cells and intact tubules. However, gross morphological changes were observed in the treated group showing inflammation with abnormal and loss of capillary tubules.

The ultrastructural examination of the rat kidney using TEM showed glomeruli with tubules (Figure 10). The glomeruli were normal with uniformly formed functional units called the tubules and its interstices containing the hematopoietic tissue (Figures 10A and 10B). The kidney tissue showed intact glomeruli with normal brush border, basement membrane and cell organelles including nuclei, mitochondria, and membranous vesicles. Further, the glomeruli also showed normal mesangial cells with normal basement membrane in the capillary tufts with few red blood cells (RBCs) in their lumen and normal surrounding primary and secondary

processes of the intact podocytes. However, significant morphological alterations were observed in the treated rats when compared with the control group (Figures 10C and 10D). The morphological changes were more prominent at 1000 mg/Kg dose of AgNPs as against the other two doses. The kidney of treated rats showed abnormal glomeruli with inflammation and loss of capillary tubules. The glomeruli showed podocytes with swollen and elongated primary and secondary processes. The renal epithelium showed a thickened basement membrane. The glomerular epithelial cells were also found to be swollen. Further, the cytoplasm showed a few mitochondria with destroyed cristae and numerous membranous vesicles and lysosomes filled with electron dense material (Figures 10E and 10F).
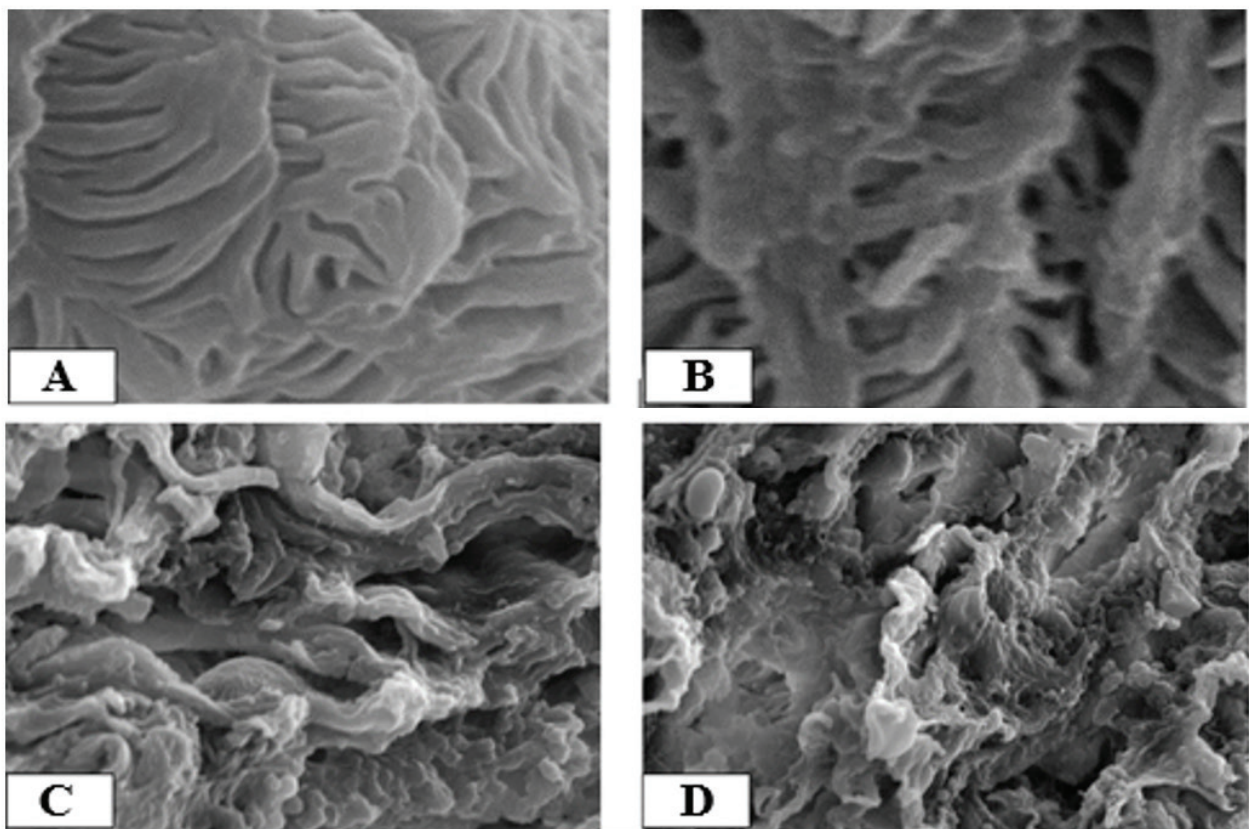
Figure 9) *Effect of silver nanoparticles on the histopathology of kidney in Wistar rats. A) Scanning Electron Micrograph of Rat Kidney (Control) showing normal glomeruli with intact capillary tubules. B) Scanning Electron Micrograph of Rat Kidney (100 mg/kg) showing inflammation with abnormal and loss of capillary tubules. C) Scanning Electron Micrograph of Rat Kidney (500 mg/kg) showing damaged bowman's capsule with tubules and glomerular tuft. D) Scanning Electron Micrograph of Rat Kidney (1000 mg/kg) showing capillary network, podocytes, and erythrocytes. Mag: 2000× Area: 40 μm.*
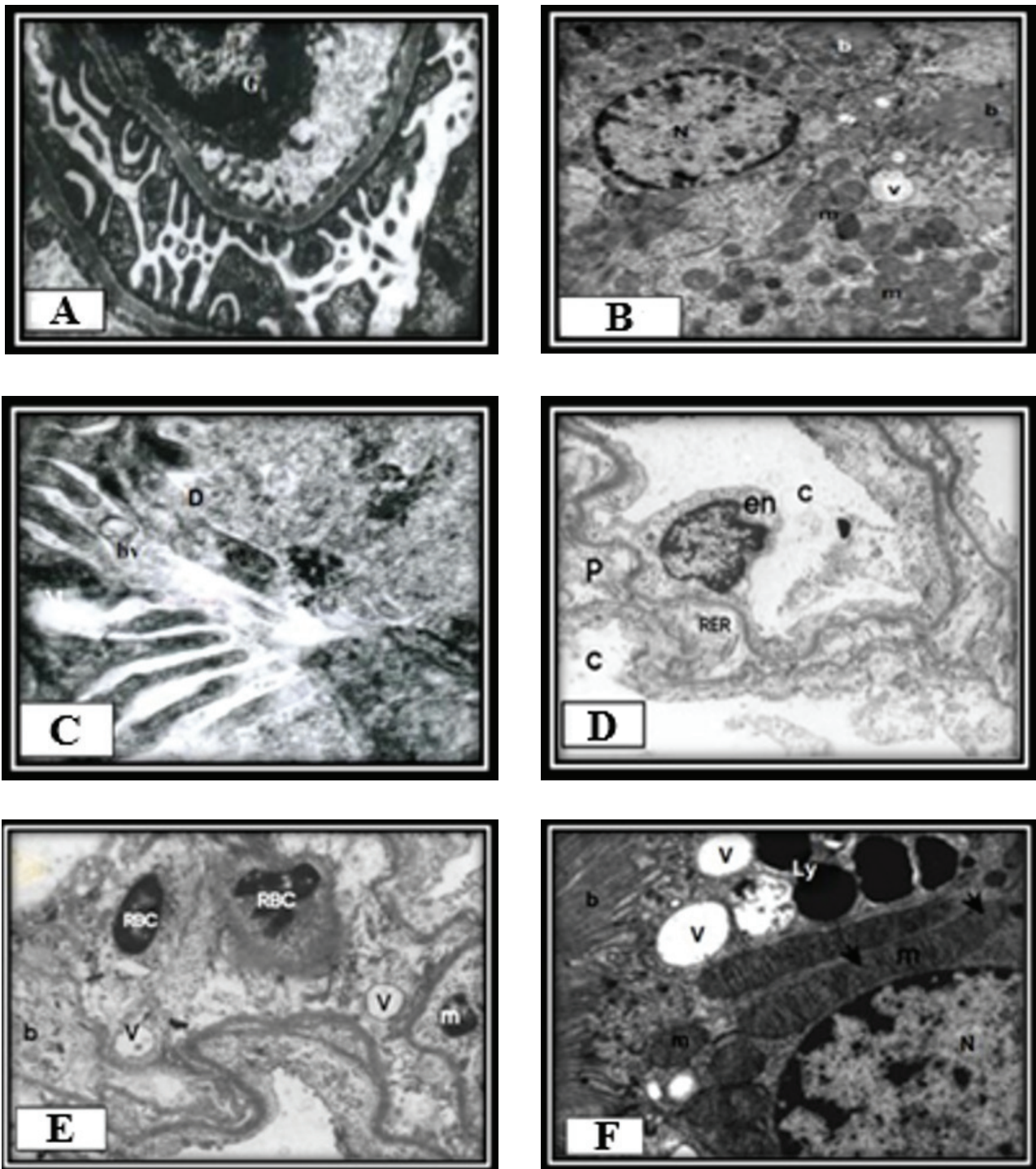
Figure 10) *Effect of silver nanoparticles on the histopathology of kidney in Wistar rats. A) Transmission Electron Micrograph of Rat Kidney (Control) showing normal glomeruli with tubules. B) Transmission Electron Micrograph of Rat Kidney (Control) showing tubular epithelial layer in the basement membrane with intact nucleus and cell organelles. C) Transmission Electron Micrograph of Rat Kidney (100 mg/kg-AgNP) showing inflammation with loss of tubules. D) Transmission Electron Micrograph of Rat Kidney (500 mg/kg AgNP) showing swollen podocytes with mitochondria, rough endoplasmic reticulum and thickening of basement membrane in the capillary tuft. E) Transmission Electron Micrograph of Rat Kidney (1000 mg/kg AgNP) showing abnormal glomeruli with swollen podocytes, thick basement membrane, RBC, s, mitochondria, and vacuoles. F) Transmission Electron Micrograph of Rat Kidney (1000 mg/kg AgNP) showing membranous vesicles, lysosomes, and mitochondria with destroyed and loss of cristae.*

G: Glomerulus; N: Nucleus; v: Vacuole; m: Mitochondria; b: Brush border; D: Debris; bv: Blood vessel; en: Endothelial cell; c: Capillary tuft; p: Podocyte; RER: Rough Endoplasmic Reticulum; RBC: Red Blood Cell; V: Vesicle; Ly: Lysosome.

Discussion

This study highlights the nephrotoxic effects induced by oral administration of Ag-NPs in Wistar rats, as evidenced by elevated levels of serum creatinine and blood urea nitrogen. Furthermore, AgNPs caused a significant increase in CAT and LPO activities, followed by a decrease in SOD and GPx activities in a dose- dependent manner. Histopathological evaluation using SEM and TEM study showed significant morphological alterations in kidneys. It has been known that nanoparticles enter the systemic circulation and then spread to the liver, spleen, and kidneys. The kidneys play a significant role as they can filter the NPs out of the systemic circulation. In doing so, they are exposed to damage via those NPs that they have filtered from the blood. Many studies on morphological, pathological as well as cellular changes from exposure to the NPs that caused renal dysfunction have been reported. Nonetheless, very few studies have discussed the potential toxic effects of NPs on renal function. The mechanism by which the nanoparticles impact the tissue or disrupt the physiological processes is through generation of reactive oxygen species [32]. The antioxidant defenses comprising of the enzymatic and non-enzymatic are very essential as they are responsible for direct removal of free radicals thus providing protection for the biological tissues including kidneys.

The present study demonstrated oral administration of AgNPs to rats had adverse effects on the antioxidant status of the kidney. The first antioxidant defense mechanism against the toxic effect of ROS in the tissues is carried out by CAT and SOD enzymes. The CAT and SOD play a prominent role in the antioxidation and elimination of ROS [33].

The conversion of superoxide radicals to H_2O_2 is executed by SOD enzyme while the CAT enzyme decomposes H_2O_2 into water and oxygen. In the present study, the increase in lipid hydroperoxides (LPO) and depletion in the GSH content were accompanied by an increase in CAT activity and a decrease in SOD activity after treatment of rats with different concentrations of AgNPs. The increase in CAT activity suggests an adaptive mechanism to reduce the toxic effects of elevated levels of H_2O_2 in the kidneys of AgNPs exposed rats. Further, an increase in the CAT activity has been correlated with the over production of H_2O_2 under stress conditions [34]. SOD enzyme is considered as the first line of defense against oxygen toxicity owing to its inhibitory effect on oxyradical formation [35]. The inhibition of SOD activity in the present study could be due to high flux of superoxide radicals resulting in H_2O_2 production in cells as advocated by [33]. Furthermore, high levels of H_2O_2 upregulate CAT activity and down regulate SOD activity as suggested by [36]. Hence, the elevation of the CAT activity in the present study could be due to its extensive involvement in the degradation of resulting H_2O_2 molecules. In the present study, the LPO activity increased significantly in the treated rats compared to control rats. The increase in LPO (Lipid hydroperoxides) in the kidney tissue of treated rats suggest enhanced lipid peroxidation to tissue damage and failure of antioxidant mechanisms to prevent the production of excess free radicals. The GPx (glutathione peroxidase) levels declined significantly in the AgNPs treated rats compared to control. GPx is important for cell survival. GPx is present in majority of the cells responsible for hydrophilic conjugation of xenobiotics and is probably the most important protective mechanism for free-radical scavenging and inhibition of xenobiotics electrophilic attack on cellular macro molecules [37]. The decline in the GPx content suggests

over utilization in the detoxification process to cope with the oxidative stress. Additionally, when excessive ROS is produced, the levels of LPO will rise and GPx levels will decline signify that the treated rats suffered severe oxidative stress conditions.

The present study also revealed elevated levels of serum creatinine and blood urea nitrogen (BUN) in treated rats compared to the control rats on administration of AgNPs. High levels of serum creatinine and blood urea nitrogen indicate improper functioning of the kidneys which could be due to several factors including kidney damage or infection and reduced blood flow to the kidneys due to shock heart failure [18]. Similar results were reported by [38] in albino rats and in Wister rats [39-41] exposed to silver nanoparticles. The results of these

biochemical markers were further supported by the histopathological evaluation of the kidney tissue using SEM and TEM studies corroborating with the results thus bearing a testimony to our present findings.

Conclusion

This study demonstrated that long-term exposure of male Wistar rats to AgNPs induced oxidative stress as evidenced by antioxidant enzyme activities with a subsequent increase in lipid peroxidation and marked morphological alteration in the exposed rats. The biochemical and structural changes were more prominent in increased dose and prolonged exposure. The study thus concludes that despite the benefits of AgNPs, it is important to test the safety of the use of different doses on vital organs such as kidneys.

References

1. Burduşel AC, Gherasim O, Grumezescu AM, et al. Biomedical Applications of silver nanoparticles: an up-to-date overview. Nanomaterials (Basel). 2018;8:681.

2. Tran QH, Le AT. Silver nanoparticles: synthesis, properties, toxicology, applications and perspectives. Adv Nat Sci: Nanosci Nanotechnol. 2013;4:033001.

3. Panacek A, Kvítek L, Prucek R, et al. Silver colloid nanoparticles: synthesis, characterization, and their antibacterial activity. J Phys Chem B. 2006;110:16248-53.

4. Rai M, Yadav A, Gade A. Silver nanoparticles as a new generation of antimicrobials. Biotechnol Adv. 2009;27:76-83.

5. Vance ME, Kuiken T, Vejerano EP, et al. Nanotechnology in the real world: redeveloping the nanomaterial consumer products inventory. Beilstein J Nanotechnol. 2015;6:1769-80.

6. Thomas K, Sayre P. Research strategies for safety evaluation of nanomaterials. Part-1: evaluating the human health implications of exposure to nanoscale materials. Toxicol Sci. 2005;87:316-21.

7. Chen X, Schluesener HJ. Nanosilver: a nanoproduct in medical application. Toxicol Lett. 2008;176:1-12.

8. Drake PL, Hazelwood KJ. Exposure-related health effects of silver and silver compounds: a review. Ann Occup Hyg. 2005;49:575-85.

9. Skvortsov AN, Ilyechova EY, Puchkova LV. Chemical background of silver nanoparticles interfering with mammalian copper metabolism. J Hazard Mater. 2023;451:131093.

10. Bergin IL, Witzmann FA. Nanoparticle toxicity by the gastrointestinal route: evidence and knowledge gaps. Int J Biomed Nanosci Nanotechnol. 2013;3:163-210.

11. Ji JH, Jung JH, Kim SS, et al. Twenty-eight-day inhalation toxicity study of silver nano particles in Sprague-Dawley rats. Inhal Toxicol. 2007;19:857-71.

12. Crosera M, Bovenzi M, Maina G, et al. Nanoparticle dermal absorption and toxicity: a review of the literature. Int Arch Occup Environ Health. 2009;82:1043-55.

13. Kim YS, Kim JS, Cho HS, et al. Twenty-eight-day oral toxicity, genotoxicity, and gender related tissue distribution of silver nanoparticles in Sprague Dawley rats. Inhal Toxicol. 2008;20:575-83.

14. Xu L, Wang YY, Huang J, et al. Silver nanoparticles: synthesis, medical applications and biosafety. Theranostics. 2020;10:8996-9031.

15. Park E, Bae E. Repeated dose-toxicity, and inflammatory responses in mice by oral administration of silver nanoparticles. Environ Toxicol Pharm. 2010;30:162-8.

16. Braydich-Stolle L, Hussain S, Schlager JJ, et al. *In vitro* cytotoxicity of nanoparticles in mammalian germline stem cells. Toxicol Sci. 2005;88:412-9.

17. L'azou B, Jorly J, On D, et al. *In vitro* effects of nanoparticles on renal cells. Part Fibre Toxicol. 2008;5:22.

18. Kermanizadeh A, Vranic S, Boland S, et al. An *in-vitro* assessment of panel of engineered nanomaterials using a human renal cell line: cytotoxicity, pro-inflammatory response, oxidative stress and genotoxicity. BMC Nephrol. 2013;14:96.

19. Al-Attar AM, AL-Taisan WA. Preventive effects of black seed (*Nigella sativa*) extract on Sprague Dawley rats exposed to diazinon. Aust J Basic Appl Sci. 2010;4:957-68.

20. Yakubu MT, Musa IF. Liver and kidney functional indices of pregnant rats following the administration of the crude alkaloids from *Senna alata* (Linn. Roxb) leaves. Iran J Toxicol. 2012;6:615-25.

21. Ferdous Z, Nemmar A. Health impact of silver nanoparticles: a review of the biodistribution and toxicity following various routes of exposure. Int J Mol Sci. 2020;21:2375.

22. Zhao H, Li L, Zhan H, et al. Mechanistic understanding of the engineered nanomaterial-induced toxicity on kidney. J Nanomater. 2019;2019:1-12.

23. https://www.oecd-ilibrary.org/environment/test-no-407-repeated-dose-28-day-oral-toxicity-study-in-rodents_9789264070684-en

24. Cho YM, Mizuta Y, Akagi JI, et al. Size-dependent acute toxicity of silver nanoparticles in mice. J Toxicol Pathol. 2018;31:73-80.

25. Wheeler CR, Salzman JA, Elsayed NM, et al. Automated assays for superoxide dismutase, catalase, glutathione peroxidase and glutathione reductase activity. Anal Biochem. 1990;184:193-9.

26. Mattiazzi M, D'Aurelio M, Gajewski CD, et al. Mutated human SOD1 causes dysfunction of oxidative phosphorylation in mitochondria of transgenic mice. J Biol Chem. 2002;277:29626-33.

27. Anderson ME. Enzymatic and chemical methods for the determination of glutathione. In: Dolphin D, Poulson R, Avramovic O (eds), Glutathione: Chemical, Biochemical and Medical Aspects, Vol-A. John Wiley and Sons. New York, USA. 1989.

28. Hayal MA. Principles and Techniques of Electron Microscopy. (4thedn), Cambridge University Press, Cambridge, UK. 2000.

29. Gluert AM. Fixation, Dehydration and Embedding of Biological Specimens: Volume 3 of Practical Methods in Electron Microscopy. North-Holland Publishing Company, Amsterdam, Netherlands. 1974.

30. Ozbez E, Ozbek A. A microscopic pathology of the liver in rats fed with Fusarium graminearum-inoculated diet. J Int Med Res. 2003;31:392-401.

31. Morris JK. A formaldehyde glutaraldehyde fixative of high osmolality for use in electron microscopy. J Cell Biol. 1965;27:1-49A.

32. Glauert AM, Lewis PR. Biological Specimen Preparation for Transmission Electron Microscopy. Princeton University Press, Princeton University, USA. 2014.

33. Awasthi KK, John PJ, Awasthi A, et al. Multi-walled carbon nanotubes induced hepatotoxicity in Swiss albino mice. Micron. 2013;44:359-64.

34. Jihen EH, Imed M, Fatima H, et al. Protective effects of selenium (Se) and Zinc (Zn) on cadmium (Cd) toxicity in the liver of rats: effects of the oxidative stress. Ecotox Environ Saf. 2009;72:1559-64.

35. Islam F, Yasmeen T, Ali Q, et al. Influence of Pseudomonas aeruginosa as PGPR on oxidative stress tolerance in wheat under Zn stress. Ecotoxicol Environ Saf. 2014;104:285-93.

36. Li ZH, Li P, Randak T. Effect of a human pharmaceutical carbamazepine on antioxidant responses in brain of a model teleost *in vitro:* an efficient approach to biomonitoring. J Appl Toxicol. 2010;30:644-8.

37. Fernández-Urrusuno R, Fattal E, Féger J, et al. Evaluation of hepatic antioxidant systems after intravenous administration of polymeric nanoparticles. Biomaterials. 1997;18:511-7.

38. Al-Attar AM. Antioxidant effect of vitamin E treatment on some heavy metals-induced renal and testicular injuries in male mice. Saudi J Biol Sci. 2011;18:63-72.

39. Sarhan OM, Hussein RM. Effects of intraperitoneally injected silver nanoparticles on histological structures and blood parameters in the albino rat. Int J Nanomedicine. 2014;9:1505-17.

40. Tiwari DK, Jin T, Behari J. Dose-dependent *in-vitro* toxicity assessment of silver nanoparticle in Wistar rats. Toxicol Mech Methods. 2011;21:13-24.

41. Olugbodi JO, Lawal B, Bako G, et al. Effect of sub-dermal exposure of silver nanoparticles on hepatic, renal and cardiac functions accompanying oxidative damage in male Wistar rats. Sci Rep. 2023;13:10539.